Spatial Localization of Chaperone Distribution in the Endoplasmic Reticulum of Yeast

Marc Griesemer[1], Carissa Young[2], Anne Robinson[2], and Linda Petzold[1]

[1]Department of Computer Science, University of California, Santa Barbara, CA 93106
[2]Department of Chemical Engineering, University of Delaware, Newark, DE 19716

Abstract

In eukaryotes, the endoplasmic reticulum (ER) serves as the first membrane-enclosed organelle in the secretory pathway, with functions including protein folding, maturation, and transport. Molecular chaperones, of the Hsp70 family of proteins, participate in assisting these processes and are essential to cellular function and survival. BiP is a resident Hsp70 chaperone in the ER of *Saccharomyces cerevisiae*. In this study we have created a partial differential equation (PDE) model to examine how BiP interacts with the membrane-bound co-chaperone Sec63 in translocation, a process in which BiP assists in guiding a nascent protein into the ER lumen. We found that when Sec63 participates in translocation through localization at the membrane, the spatial distribution of BiP is inhomogeneous, with more BiP at the surface. When translocation is inhibited through a disabling of Sec63's membrane tether, the concentration of BiP throughout the ER becomes homogeneous. Our computational simulations suggest that Sec63's localization and the resulting binding to BiP near the membrane surface of the ER enable a heterogeneous distribution of BiP within the ER, and may facilitate BiP's role in translocation.

1 Introduction

Molecular chaperones participate in a wide range of processes essential to cellular function and survival. Found in all organisms, and ubiquitously distributed in the major compartments of eukaryotic cells, most are intricate players in the response to cellular stress [1]. Hsp70s assist in protein folding and maturation, assembly or disassembly of complexes, ribosomal RNA processing, translocation of newly synthesized proteins, suppression of aggregation, and protein degradation (as reviewed in [2, 3]). The versatility among molecular chaperones is intriguing, for they have a single purpose: to bind protein substrates. The very high degree of conservation among Hsp70 proteins may favor a unique molecular mechanism common to all, whereas functional differences may depend on modulating co-chaperones such as Hsp40s and nucleotide exchange factors (NEFs) [4]. This phenomenon of a protein having multiple, sometimes competing functions, indicates a high level of systems control.

In the lumen of the endoplasmic reticulum (ER), a network of chaperones and cofactors ensures the proper folding of secretory proteins. One of the most abundant proteins of the ER is the Hsp70 molecular chaperone, BiP. Through biochemical and genetic experiments, BiP has been identified in critical cellular processes including protein translocation of newly synthesized precursors across the ER membrane, folding and maturation, karyogamy, and ERAD (ER-associated degradation) where unfolded or abnormally folded proteins are sent back to the cytosol for degradation [5–9]. Like other Hsp70 chaperones, BiP assists the folding of a protein by repeated ATP-controlled cycles of binding and release. Co-chaperones, such as Hsp40s, stimulate the binding of molecular chaperones to the substrate and regulate chaperone activities [10]. In the ER of *S. cerevisiae*, co-chaperone Sec63 directly interacts with BiP, increasing its affinity for the nascent proteins proceeding through the translocation pore [11–13] (Figure 1). Simultaneously within the ER lumenal environment, co-chaperones Scj1 and Jem1 associate with BiP during the processes of protein maturation

and karyogamy, respectively [8, 9, 14]. BiP, Jem1, and Scj1 are all involved in the degradation of aberrant soluble proteins through ERAD [15]. As illustrated in Figure 1, Sil1 and Lhs1 are the nucleotide exchange factors (NEF) that play key roles in these processes by triggering substrate release [16, 17].

The regulation of Hsp70-Hsp40-NEF interactions is best understood for *Escherichia coli* homologues DnaK, DnaJ, and GrpE. Mechanistic details have been experimentally explored and mathematically modeled [18–24]. Yet, *E. coli* is an organism that does not consist of membrane-bound compartments to perform distinct cellular functions. Additionally, many chaperone-mediated processes involve spatial aspects, such as the subcellular localization of messenger RNA leading to translation of their encoded proteins [25]; subcompartments of the nucleus implicated in the processes of transcription and splicing [26, 27]; and the spatial localization of BiP at the ER membrane maintaining the permeability barrier during protein translocation [28].

Yeast, *S. cerevisiae*, is a simple eukaryotic organism that compartmentalizes selective processes and protein-protein interactions to specified organelles. Proteomic studies have verified the location of ER-resident proteins of *S. cerevisiae* and identified absolute levels of protein expression [29, 30]. These data suggest that the concentration of BiP exceeds the level of co-chaperones by at least an order of magnitude at normal growth conditions, and is significantly up-regulated during quality control mechanisms of the cell including the heat shock response (HSR) and unfolded protein response (UPR) [31, 32]. It is also known that multiple BiPs can bind to substrates with varying affinities [33]. Experimentally, the co-chaperone Sec63 must be spatially localized at a suborganelle level – the ER membrane – in order for translocation to occur [34]. Given this evidence, we hypothesize that the spatial localization of BiP and interactions with co-chaperones regulate its diversity and functionality in the ER of *S. cerevisiae*.

Thus, we describe our model development in Section 2, discuss the significance of our simulations in Section 3, and examine the sensitivity of our model

to parameter perturbations in Section 4. In order to investigate the chaperone and co-chaperone interaction of BiP and Sec63, respectively, in ER translocation, we have introduced spatial components to our model. Subsequently, we have shown that Sec63's localization and functional interaction with BiP in translocation provides an explanation for BiP's heterogeneity in the ER.

2 Models

Modelers have attempted to discern the role of Hsp70 chaperones in assisting and accelerating translocation of proteins across membranes of organelles, specifically the ER and mitochondria of *S. cerevisiae*. Previous work has focused on transport mechanisms, including either the Brownian ratchet model [35], comparison to the power stroke model [36, 37], or a unifying mechanism of both termed entropic pulling [4]. We have examined the significance of spatial effects between BiP and the ER membrane co-chaperone Sec63 and implemented the reaction rates associated with previous models that evaluate a nascent protein as it transits through the translocation pore. Specifically, we are interested in how the BiP-Sec63 interaction enhances translocation of the nascent protein. Experiments exploring the BiP-Sec63 interaction *in vitro* suggest that Sec63 acts as an anchor to localize BiP within the proximity of the translocation channel, and accelerates the transit of a peptide through the membrane pore by regulating ATP hydrolysis of the chaperone [5, 34].

This work implements the experimental evidence [12, 16, 17, 38–42] with the added spatial component including the ER membrane and lumenal regions. Developing spatially-relevant models is important as *in vivo* experiments such as single particle tracking (SPT) and technology advancements in fluorescence imaging begin to capture spatial effects of protein localization (reviewed in [43]). Estimates of species concentrations have been determined for *S. cerevisiae* [30] as well as binding affinities between BiP, Sec63, and synthetic peptides [38, 39]. When experimental data was not available, as in the case of the interactions

between NEFs, Sil1 and Lhs1 and BiP, established estimates from the mammalian literature were used (Supplementary Material). However, a degree of uncertainty is inherent when evaluating kinetic rates as a result of *in vitro* experiments. We have incorporated these estimates into models used to elucidate *in vivo* mechanisms and varied the parameters by two orders of magnitude to test the sensitivity of the particular values. Due to the high degree of homology between chaperones and co-chaperones amongst eukaryotes, we believe that this estimation procedure is an appropriate method.

Our goal is to use modeling to better understand the role of Sec63 in partitioning of BiP within the ER. To this end, we first constructed an ODE model to examine the reaction pathways and then extended this system to a PDE model in order to capture the spatiotemporal dynamics.

2.1 Model Descriptions

2.1.1 Core ODE model

Our core model is described by a system of ordinary differential equations. It is a 7 state, 13 parameter model representing the interactions of BiP with the co-chaperone Sec63 and unfolded proteins. The schematic below, Figure 2, depicts all plausible states of BiP binding to nascent proteins during protein translocation into the ER lumen. In general, molecular chaperones alternate between an ATP-bound state representing fast substrate binding/release rates and therefore a low affinity for proteins (upper right triangle, Fig.2), and an ADP-bound state characteristic of slow association/dissociation kinetics and a high affinity for substrates (lower left triangle, Fig. 2) [44]. The states of the model are given in Table 1.

Under physiological conditions, BiP preferentially binds to ATP (X_1) and associates with either unfolded proteins in the lumen or nascent proteins of the translocon (Fig. 1). BiP's interaction with unfolded proteins can occur in the presence or absence of co-chaperone mediation ($X_1 \rightarrow X_6$) [38, 40] where BiP

preferentially binds to hydrophobic residues [33, 45]. ATP hydrolysis ensues ($X_6 \rightarrow X_7$), trapping the peptide to form X_7. Due to low intrinsic rates of bound peptide released from the chaperone complex, nucleotide exchange factors further accelerate the cycle of protein folding ($X_7 \rightarrow X_5 \rightarrow X_1$). The conventional mechanism of translocation proceeds with the binding of the co-chaperone Sec63 to BiP (X_2) which synergistically stimulates peptide binding (X_3) and ATP hydrolysis (X_4). This coupling effect has been shown to mediate the molecular trapping of proteins that BiP would not bind on its own [38, 39]. However, it is also plausible that BiP could initially bind to the unfolded protein and then sequentially associate with its co-chaperone during translocation. This scenario is represented in states $X_1 \rightarrow X_6 \rightarrow X_3$.

We have assumed that a single BiP is activated per Sec63 molecule located at the ER membrane. *In vitro* studies have indicated that the BiP-Sec63 interaction occurs transiently, and suggest that one Sec63 molecule could potentially activate at least ten BiP molecules [38]. On average, *E. coli* experiments have determined that incoming proteins present a new Hsp70 binding site every 25 to 35 amino acids [46] which is consistent with *S. cerevisiae* literature that estimates a minimum of six to seven molecules of BiP bound to the endogeneous protein, ppαF [47]. For simplicity, our model assumes a 1:1 stoichiometry between BiP and unfolded proteins as well as between BiP and Sec63.

Simulations were realized until the values reached a steady-state level and then the final species concentrations were obtained for a range of initial conditions. We found that when the total amount of BiP is low, the Sec63-dependent pathway (Fig. 2, outer loop) accounted for most of the bound BiP. As the total amount of BiP in the system was increased, the Sec63-dependent pathway (Fig. 2, diagonal) dominated, and states such as BiP-U-ATP (X_6) accounted for most of the BiP. The latter result confirmed an important point: that BiP strongly interacts with unfolded protein, although it should be mentioned that the association rate to form X_6 was chosen on the higher end of the range of experimental data [24]. This core ODE model served as a description of reaction

kinetics between BiP, Sec63, and unfolded protein, and was a building block for constructing a spatially-dependent model describing chaperone interactions in the ER. Details of the model are summarized in the Supplementary Material.

2.1.2 PDE Model

We constructed a PDE model, making use of the reaction kinetics from the ODE model, to determine the spatial distribution of BiP in the ER. The model incorporates: (1) chemical reactions representing transitions between states in the ODE system that take place on the inner membrane, and (2) diffusion into the lumen of the ER. This spatially dependent system of equations was approximated by the method of finite differences (Figure 3). The irregular geometry of the ER was simplified to a sphere (surrounding a spherical nucleus) and assumed to be symmetric. With these assumptions, the (time-dependent) system can be modeled in one spatial dimension. We believe a PDE model is justified because BiP and (wild-type) Sec63 have a localized interaction at the membrane that precludes a well-mixed system.

We define the membrane-associated zone as the membrane portion of the ER where protein-protein interactions take place between BiP and the other proteins in the system. Images attained by electron microscopy (EM) show that the membrane has a defined thickness [48], shown as 35 nm in Figure 3. Sec63 spans the membrane [49] and associates with the Sec61-constituted pore channel [50]. We do, however, consider the entire region as well-mixed, represented by the boundary condition of the PDE.

The rate of change of the concentration of species k is the sum total of the concentrations of the free and bound species plus the diffusion in the interior.

$$\frac{\partial C_{z,k}}{\partial t} = R_k + D\frac{\partial^2 C_{l,k}}{\partial x^2}\Big|_{x=0} \tag{1}$$

Reactions and (one-dimensional) diffusion occurs in the lumen

$$\frac{\partial C_{l,k}}{\partial t} = R_k + D\frac{\partial^2 C_{l,k}}{\partial x^2} \tag{2}$$

with the nuclear-ER boundary condition given by

$$\frac{\partial C_{l,k}}{\partial x}\Big|_{x=L_l} = 0. \tag{3}$$

Here, $C_{z,k}$ is the membrane-associated zone concentration and $C_{l,k}$ represents the concentration in the lumen for diffusing species k. If this species exists only in the membrane-associated zone, then this term is absent. D is the diffusion coefficient (assumed to be the same for all ER lumenal species), and R_k is the reaction term for species k. L_z is the length of the membrane-associated zone (in one dimension), and L_l is the annular radius of the lumen. The variable x represents the distance from the membrane-associated zone for a particular point on the grid.

Discretizing in space, we obtain

$$\frac{\partial (C_{z,k})}{\partial t} = R_k + D\frac{C^1_{l,k} - C_{z,k}}{\Delta x^2} \tag{4}$$

$$\frac{\partial C^1_{l,k}}{\partial t} = R_k + D\frac{C_{z,k} - 2C^1_{l,k} + C^2_{l,k}}{\Delta x^2} \tag{5}$$

$$\vdots$$

$$\frac{\partial C^N_{l,k}}{\partial t} = D\frac{C^{N-1}_{l,k} - C^N_{l,k}}{\Delta x^2}, \tag{6}$$

where $C^i_{l,k}$ represents the concentration of species k at grid point i in the lumen, and Δx is the spatial separation between two consecutive grid points. The boundary at $x = 0$ is the ER membrane, and the boundary at $x = L_l$ is the nucleus. Given this formulation, the concentration of each species is tracked spatially and temporally.

Several assumptions were made to simplify the model and approximate the

dynamics of the system. Reactions can occur in both the membrane-associated zone and the lumen. We define unfolded proteins as one species without distinguishing between proteins diffusing in the lumen from those transiting the translocation pore. Loss of proteins at the translocon (due to completed translocation) is offset by a production reaction ($\emptyset \rightarrow U$) that allows for replenishment of the U pool. The translocated U is designated as a non-reacting product U_t (Figure 2). Thus, the total amount of unfolded protein in the model remains constant.

3 Simulation Results

3.1 Model Scenarios

Three scenarios were constructed to simulate different conditions in the ER. In each scenario, different species were allowed to diffuse in the lumen. In our model, we assume that if all the constituent species in a bound state can diffuse in a particular scenario, then the bound state can diffuse as well. The scenarios are:

(1) The wild-type case that assumes that ER-resident chaperone BiP, nucleotide exchange factors Sil1 and Lhs1, soluble U, and selective complexes, diffuse freely throughout the lumen [16, 41, 51, 52]. Sec63 is an integral membrane protein and therefore remains embedded in the ER lipid bilayer [53].

(2) In addition to the species outlined in Scenario 1, Sec63 and membrane-associated complexes are now allowed to diffuse into the lumen. Experimental data has shown that the presence of a soluble variant of Sec63 (63Jp) not localized to the ER membrane inhibits efficient protein translocation. These results suggest that 63Jp competes with the endogenous membrane-localized Sec63 by sequestering BiP from the vicinity of the translocon pore (Sec61 complex of Fig. 1) [34]. In this case, we can test

whether the variant's ability to diffuse into the lumen leads to a loss of BiP's heterogeneous distribution in the ER.

(3) When the BiP-Sec63 protein interactions are severely impaired, or in the absence of Sec63 within the system of scenario 1 (i.e. zero concentration), we have been able to mimic a situation in which ER protein translocation fails. Mutations in either Sec63 or BiP have been shown to inhibit translocation due to defects in Sec63 interacting with BiP (sec63-1, [5, 54]) and, to varying degrees, BiP mutants display different translocation efficiencies into the lumen (kar2-113, kar2-159, and kar2-203; [55]).

It should be noted that only scenario one represents physiological conditions. Scenarios 2 and 3 are special conditions that have been experimentally obtained using either protein variants or thermosensitive yeast strains. The species and states that diffuse in each scenario are given in Table 2.

3.2 Ratio Metric

From the ER PDE model, we determined the ratio of total BiP concentration localized to the membrane-associated zone compared to the total BiP concentration of the interior. This metric gives an indication of BiP's spatial localization within the ER sub-compartments. The default scenario is to tether Sec63 to the membrane, while BiP, NEF and U are allowed to diffuse. From these scenarios, one can make predictions of the importance of these species on translocation. This is described by the equation:

$$Ratio_{BiP} = \frac{\left[BiP_{total}\right]_z}{[BiP_{total}]_l}, \tag{7}$$

where the subscript z means the membrane-associated zone and l means the lumen. At steady-state, the concentrations of diffusing species in the membrane-associated zone and the lumen are the same, with the concentration of the non-diffusing species on the membrane-associated zone determining the divergence of the BiP ratio from unity.

3.3 Model Results

Using the DASPK ODE/DAE solver [56], we ran simulations for each of the scenarios until steady-state ($t = 10^5$ s). The system starts from conditions where all proteins are free and present in the membrane-associated zone. Diffusion is fast, equalizing gradients across the ER. Reactions then occur in the membrane-associated zone and in the lumen on a slower time scale. We analyzed the concentration of each state in the membrane-associated zone and at interior grid points and then calculated the ratio of total BiP concentration in the membrane-associated zone compared to the total BiP concentration in the lumen. Simulations accounted for total Sec63 ranging from 0.55 to 1.37 mM (10,000-25,000 molecules) while BiP and NEF concentrations were varied from 0.55 to 55 mM (10^4-10^6 molecules). These initial conditions were based on a range around populations given in the Yeast Genome Database [30]. The amount of total unfolded protein (U) was 5.5 mM or 10^5 molecules (in Section 4, Sensitivity Analysis).

When Sec63 is appropriately integrated in the membrane, BiP preferentially remains in the membrane-associated zone (Figure 4), resulting in an inhomogeneous distribution throughout the ER. This is expected from the model since BiP is reacting in the membrane-associated zone and forming non-diffusing species. When Sec63 is allowed to diffuse or is removed from the system entirely, BiP is uniformly distributed in the ER, resulting in a BiP ratio (Equation 7) of one for all total values of Sec63 and BiP. Thus, when translocation is inhibited, the concentration is homogeneous. When total BiP levels are low, most of it is involved in translocation, so the BiP ratio is high (left side of Fig. 4 graph). In the limit of high BiP levels, relatively less BiP is used in translocation, so its distribution tends towards homogeneity (right side of Fig. 4 graph). This calculation was initially performed with 11 spatial grid points and repeated for several grid sizes in order to increase the resolution of our results (e.g. up to 1000), yielding identical results for the ratios.

We examined the results of an ODE model to describe the impact of the

interaction between BiP and Sec63 on the chaperone distribution in the ER. In this model, we assumed that fast diffusion produced a well-mixed system for all species. We then scaled the concentrations of Sec63-derived states (i.e. X2, X3, and X4) with respect to the volume of the membrane-associated zone and the concentrations of the remaining states using the combined volume of the membrane zone and lumen. The calculation of the BiP ratio then proceeded as defined in the last section.

In comparison with the PDE model, we found that this modified ODE model resulted in a higher BiP ratio at low total BiP populations as shown in Figure 4. This discrepancy occurs because in the ODE model, Sec63 has access to the entire BiP population for translocation. The PDE model, on the other hand, allows for the presence of BiP in both the membrane-associated zone and the lumen. In this case, a percentage of BiP does not participate with Sec63 in translocation. Especially when BiP is scarce, this difference produces a higher BiP ratio in the ODE model versus the PDE model. Given BiPs known presence in both membrane-associated zone and in the lumen, we believe that a spatial model best describes the chaperone dynamics in the ER. Furthermore, the PDE model takes into account that the lumenal BiP is involved in other processes (e.g. protein folding and degradation).

The determination of an actual physiological value of the BiP ratio in Figure 4 is complicated; many cellular factors affect it. For example, if BiP binds at higher stoichiometric ratios to Sec63 and U than 1:1, then there would be much more BiP found in the membrane-associated zone, and the BiP ratio would increase for the same initial conditions. BiP is involved in multiple non-translocation cellular functions [57], which may result in a smaller percentage available to translocation, and would describe the right side of Figure 4. If either BiP or Sec63 are partially defective in their interaction with each other [39, 58], this scenario would lead to a flattening of the curves toward homogeneity. Additionally, perturbations to the cellular environment, such as the induction of stress conditions in the ER lead to membrane expansion [59] and a resulting

increase in ER volume [60], yet simultaneously, the unfolded protein response (UPR) increases the amount of BiP in the lumen to handle an unfolded protein load [32]. Thus, the BiP ratio would change dynamically in time. This project does not attempt a thorough investigation of protein folding in the ER nor perturbations to the system that, in turn, induce various quality control mechanisms; rather our model introduces the effect of dimensionality — specifically ER compartmentalization — and shows that BiP's interaction with Sec63 at the membrane brings about spatial localization in the chaperone's distribution within the ER, which will ultimately have implications in protein folding and other ER-related functions.

4 Sensitivity Analysis

Although we found BiP's concentration in the ER under wild-type conditions to be inhomogeneous (scenario 1), we also wanted to examine how the degree of heterogeneity (as quantified in the BiP ratio) would change under variation in model parameters and initial conditions, to examine the influence of various model inputs on the system.

We first simulated the variation in total number of each protein species in the ER. The Yeast Genome Database reports the total physiological population of BiP and Sec63 proteins at $337,000$ and $17,700$ molecules, respectively, but with those estimates there is a great deal of uncertainty. It is known that BiP levels in the yeast ER can fluctuate and are regulated by the unfolded protein response. Cellular conditions also dictate a large possible range in concentration of unfolded proteins. Thus we simulated the model over a large range of values for all protein species, as summarized in Table 3. The resulting BiP ratio for variation in Sec63 is given in Figure 4. We also examined a range of unfolded protein concentrations in our simulations from 0.55 to 8.25 mM (10,000-150,000 molecules). The ratio results for U are shown in Figure 5. An estimate for U came from Surface Plasmon Resonance (SPR) experiments [39] using the peptide

p5 at $2\,mM$ or roughly $40,000$ molecules in the ER. We found that this value of protein concentration resulted in less than a one percent deviation in the BiP ratio from our standard conditions (at $5.5\ mM$ or $100,000$ molecules). Most of the U binds with free BiP, but the vast excess remains free and is not a factor of the BiP ratio calculation. Overall, our simulations with the aforementioned Sec63 and U concentrations have confirmed our previous result that when BiP levels are low, the BiP ratio is high and is affected by the amount of Sec63 in the system. As BiP levels are increased, the BiP ratio becomes insensitive to changes in all initial conditions.

We next considered the binding rate between BiP and U as variable parameters (kinetic parameters k_2 and k_7 , Figure 6). BiP interacts with varying affinities to numerous types of unfolded proteins in the ER and these interactions are dependent on the exposed hydrophobic residues of the unfolded proteins [45]. Multiple BiPs can bind to a single translocating protein resulting in stoichiometric effects on the reaction, impacting the overall rate as well [35]. We varied the association rates over five orders of magnitude and recorded the BiP ratio for each simulation. As the association rate between BiP and U increases, there is less of these species in the free (as opposed to bound) state, but this does not affect the total amount of BiP bound to Sec63 at the membrane. Therefore, we found that the BiP ratio was essentially the same for all kinetic values.

We examined the effect on the BiP ratio given a change in the Sec63 dissociation rate from the trimeric complex of BiP, Sec63, and U (Figure 7). This is described by the kinetic rate constants k_5 and k_{-3}. The values from the literature are 0.0086 and 0.038 s^{-1} [38], respectively. Rate k_5 is slower than the reactions upstream and downstream in the pathway (e.g., $k_4 = 0.016\ s^{-1}$ and $k_6 = 0.267\ s^{-1}$). Thus, a bottleneck occurs, resulting in a high concentration of the BiP-Sec63-U-ADP (X_4) state. *In vitro* experiments [39, 61, 62] suggest that Sec63 may have a more transient interaction with BiP, which would allow for higher translocation efficiency. We increased the Sec63 dissociation rate ten, one hundred, and a thousand fold, and found that the BiP ratio decreased at

low levels of BiP and Sec63. We surmise this is due to translocating protein being shuttled out of the Sec63-dependent pathway at a faster rate, which in the wild-type scenario accounts for the excess BiP on the membrane.

These results were also verified by local sensitivity analysis. Using SUNDIALS [63], we computed the sensitivities of the BiP ratio to perturbations of the reaction-rate parameters. If the BiP ratio is defined as a function G, by the chain rule we get the derived function,

$$\frac{dG}{d\mathbf{p}} = \frac{\partial G}{\partial \mathbf{C}} \frac{\partial \mathbf{C}}{\partial \mathbf{p}} + \frac{\partial G}{\partial \mathbf{p}} \tag{8}$$

where $\mathbf{C}$ and $\mathbf{p}$ represent the states and parameters, respectively. The derivative $\partial \mathbf{C}/\partial \mathbf{p}$ is the standard sensitivity matrix while the second term $\partial G/\partial \mathbf{p}$ equals zero because the BiP ratio has no explicit dependence on parameters. The BiP ratio sensitivities are then scaled by the BiP ratios and parameter values to allow for comparison. The results are summarized in Table 4.

We took the minimum and maximum of 13 sets of initial conditions as defined in the last section as the range of our sensitivities. We then ranked the parameters by their maximum and calculated the mean of the ensemble. As Table 4 illustrates, the BiP ratio is robust to perturbations in parameters.

Finally, we examined the sensitivity of the BiP ratio by varying all the kinetic parameters simultaneously. We used uniform random numbers to select each parameter value in the range $[0.1p_i,\ 10p_i]$, where p_i is the nominal value of the parameter. From this method, we generated 10^5 sets of parameters to serve as the input for the simulations. We then simulated the model, increasing the total BiP concentration from 0.55 to 55 mM, and recording the resulting distributions of the BiP ratio in a histogram as presented in Figure 8. Other metrics were considered [64], but we wanted to examine the global sensitivity of the BiP ratio and to vary more than one parameter at a time.

We found that at the low end of the BiP concentration range (0.55 mM), the BiP ratio had a wide spread of values for the simulations. When BiP is scarce,

changes in kinetic parameters have a significant effect on whether the BiP is bound to Sec63 at the membrane or diffuses freely in the lumen. Despite this sensitivity, most simulations yielded a highly heterogeneous BiP distribution (BiP Ratio = 3.5-163.7, 95 percent confidence interval for total BiP = 0.55 mM), confirming that most of the BiP participates in translocation. The tails of the BiP ratio distributions are due to the combination of parameters all being near their maximum values. As the total BiP in the ER increases, more of the BiP is not interacting with Sec63 (but rather freely diffusing in the lumen); thus the reaction parameters have much less effect. Further studies concluded that no one parameter dominates the variation of the BiP ratio. The qualitative behavior of the model was reproduced in all 10^5 simulations.

In summary, the BiP distribution is heterogeneous with a high concentration of BiP near the membrane for the wild-type condition where Sec63 is tethered to the membrane. In contrast, for situations where Sec63 is allowed to freely diffuse into the lumen, the BiP concentration is homogeneous. Is Sec63 recruiting BiP to the membrane? In the model there is no driving force for BiP diffusion toward the membrane. However, BiP has a relatively fast diffusion rate, which means that a BiP molecule readily traverses both the lumen and the membrane-associated zone. When it arrives at the membrane-associated zone, it has a high probability of binding to Sec63 and this binding results in a preferential localization at the membrane. This supports the model that the J-domain co-chaperones act to modulate BiP localization in the ER.

5 Conclusion

We have developed a spatial PDE model describing the chaperone activity in the ER of *S. cerevisiae* through reaction-diffusion equations. From the simulations, we found that the concentration of BiP in the system was inhomogeneous, with the concentration being greater on the membrane, particularly as BiP levels in the ER decrease. Our simulations showed, however, that when Sec63 was

untethered and allowed to diffuse freely into the lumen, the BiP distribution was homogeneous. This is consistent with the absence of BiP (translocation failure) at the membrane observed experimentally in this situation. Sec63's localization and functional interaction with BiP in translocation provides an explanation for BiP's heterogeneity in the ER.

6 Acknowledgements

The authors gratefully acknowledge funding from NIH Grant GM07529 and NSF IGERT Grant DGE02-21715. We also would like thank David Raden (U. Delaware) and Theresa Yuraszeck (UC Santa Barbara) for helpful discussions.

References

[1] Georgopoulos, C. and Welch, W.: 'Role of the Major Heat Shock Proteins as Molecular Chaperones', Annu. Rev. Cell Biol., 9, 1993, pp. 601–634

[2] Mayer, M. P. and Bukau, B.: 'Hsp70 Chaperones: Cellular Functions and Molecular Mechanisms', Cell Mol. Life Sci., 62, 2005, pp. 670–684

[3] Buck, T., Wright, C., and Brodsky, J.: 'The Activities and Function of Molecular Chaperones in the Endoplasmic Reticulum', Seminars in Cell and Developmental Biology, 18, 2007, pp. 751–761

[4] de los Rios, P., Ben-Zvi, A., Slutsky, O., Azem, A., and Goloubinoff, P.: 'Hsp70 Chaperones Accelerate Protein Translocation and the Unfolding of Stale Protein Aggregates by Entropic Pulling', Proc. Natl. Acad. Sci., 103, 2006, pp. 6166–6171

[5] Brodsky, J. L. and Schekman, R.: 'A Sec63p-BiP complex from Yeast is Required for Protein Translocation in a Reconstituted Proteoliposome', J. Cell Biol., 123, (6 Pt 1), 1993, pp. 1355–1363

[6] Latterich, M. and Schekman, R.: 'The Karyogamy Gene KAR2 and Novel Proteins are Required for ER-Membrane Fusion', Cell, 78, (1), 1994, pp. 87–98

[7] McCracken, A. A. and Brodsky, J. L.: 'Evolving Questions and Paradigm Shifts in Endoplasmic Reticulum-Associated Degradation (ERAD)', BioEssays, 25, (9), 2003, pp. 868–877

[8] Nishikawa, S. and Endo, T.: 'The Yeast Jem1p is a DnaJ-like Protein of the Endoplasmic Reticulum Membrane Required for Nuclear Fusion', J. Biol. Chem., 272, (20), 1997, pp. 12889–12892

[9] Schlendstedt, G., Harris, S., Risse, B., Lill, R., and Silver, P.: 'A Yeast DnaJ Homologue, Scj1p, Can Function in the Endoplasmic Reticulum with BiP/Kar2 via a Conserved Domain that Specifies Interactions with Hsp70s', J. Cell Biol., 129, 1995, pp. 979–988

[10] Hennessy, F., Nicoll, W., Zimmermann, R., Cheetham, M., and Blatch, G.: 'Not all J Domains are Created Equal: Implications for the Specificity of Hsp40-70 Interactions', Prot. Sci., 14, 2005, pp. 1697–1709

[11] Scidmore, M. A., Okomura, H. H., and Rose, M.: 'Genetic Interactions between KAR2 and SEC63, Encoding Eukaryote Homologues of DnaK and DnaJ in the Endoplasmic Reticulum', Molecular Biology of the Cell, 4, 1993, pp. 1145–1159

[12] Lyman, S. K. and Schekman, R.: 'Interaction between BiP and Sec63 is Required for the Completion of Protein Translocation into the ER of *Saccaromyces cerevisiae*', J. Cell Biol., 131, (5), 1995, pp. 1163–1171

[13] Young, B., Craven, R., Reid, P., Willer, M., and Stirling, C.: 'Sec63p and Kar2p are Required for the Translocation of SRP-dependent Precursors into the Yeast Endoplasmic Reticulum in vivo', EMBO J., 20, 2001, pp. 262–271

[14] Silberstein, S., Schlenstedt, G., Silver, P., and Gilmore, R.: 'A Role of the DnaJ Homologue Scj1 in Protein Folding in the Yeast Endoplasmic Reticulum', J Cell Biol., 143, 1998, pp. 921–933

[15] Nishikawa, S. I., Fewell, S. W., Kato, Y., Brodsky, J. L., and Endo, T.: 'Molecular Chaperones in the Yeast Endoplasmic Reticulum Maintain the Solubility of Proteins for Retrotranslocation and Degradation', J. Cell Biol., 153, (5), 2001, pp. 1061–1070

[16] Tyson, J. and Stirling, C.: 'LHS1 and SIL1 Provide a Lumenal Function that is Essential for Protein Translocation into the Endoplasmic Reticulum', EMBO J., 19, 2000, pp. 6440–6452

[17] Steel, G., Fullerton, D., Tyson, J., , and Stirling, C.: 'Coordinated Activation of Hsp70 Chaperones', Science, 303, 2004, pp. 98–101

[18] Gisler, S. M., Pierpaoli, E. V., and Christen, P.: 'Catapult Mechanism Renders the Chaperone Action of Hsp70 Unidirectional', J. Mol. Biol., 9, 1998, pp. 833–840

[19] Mayer, M. P., Schröder, H., Rüdiger, S., Paal, K., and Bukau, B.: 'Investigation of the Interaction between DnaK and DnaJ by Surface Plasmon Resonance Spectroscopy', J. Mol. Biol., 289, 1999, pp. 1131–1134

[20] Mayer, M. P., Schröder, H., Paal, K., and Bukau, B.: 'Multistep Mechanism of Substrate Binding Determines Chaperone Activity of Hsp70', Nat. Struct. Biol., 7, 2000, pp. 586–593

[21] Schmid, D., Bacci, A., Gehring, H., and Christen, P.: 'Kinetics of Molecular Chaperone Action', Science, 263, 1994, pp. 971–973

[22] Laufen, T., Mayer, M. P., Beisel, C., Klostermeier, D., Reinstein, J., and Bukau, B.: 'Mechanism of Regulation of Hsp70 Chaperones by DnaJ Cochaperones', Proc. Natl. Acad. Sci. USA, 96, 1999, pp. 5452–5457

[23] Chesnokova, L. S., Slepenkov, S. V., Protasevich, I., Sehorn, M. G., Brouillette, C. G., and Witt, S. N.: 'Deletion of DnaK's Lid Strengthens Binding to the Nucleotide Exchange Factor, GrpE: A Kinetic and Thermodynamic Analysis', Biochem., 42, 2003, pp. 9028–9046

[24] Hu, B., Mayer, M. P., and Tomita, M.: 'Modeling Hsp70-Mediated Protein Folding', Biophys. J., 91, (2), 2006, pp. 496–507

[25] Holt, C. E. and Bullock, S.: 'Subcellular mRNA Localization in Animal Cells and Why It Matters', Science, 326, (5957), 2009, pp. 1212–1216

[26] Lamond, A. I. and Earnshaw, W. C.: 'Structure and Function in the Nucleus', Science, 280, 1998, pp. 547–553

[27] Misteli, T. and Spector, D. L.: 'The Cellular Organization of Gene Expression', Curr. Opin. Cell Biol., 10, 1998, pp. 322–331

[28] Haigh, N. and Johnson, A.: 'A New Role for BiP: Closing the Aqueous Translocon Pore During Protein Integration into the ER Membrane', J. Cell Biol., 156, 2002, pp. 261–270

[29] Huh, W.-K., Falvo, J. V., Gerke, L. C., Carroll, A. S., Howson, R. W., Weissman, J. S., and O'Shea, E. K.: 'Global Analysis of Protein Localization in Budding Yeast', Nature, 425, (6959), 2003, pp. 686–691

[30] Ghaemmaghami, S., Huh, W.-K., Bower, K., Howson, R. W., Belle, A., Dephoure, N., O'Shea, E. K., and Weissman, J. S.: 'Global Analysis of Protein Expression in Yeast', Nature, 425, (6959), 2003, pp. 737–741

[31] Mager, W. H. and Herreira, P. M.: 'Stress Response of Yeast', Biochem J., 290, (Pt. 1), 1993, pp. 1–13

[32] Travers, K., Patil, C. K., Wodicka, L., Weissman, J. S., and Walter, P.: 'Functional and Genomic Analyses Reveal an Essential Coordination between the Unfolded Protein Response and ER-Associated Degradation', Cell, 101, 2000, pp. 249–258

[33] Flynn, G., Pohl, J., Flocco, M., and Rothman, J.: 'Peptide-binding Specificity of the Molecular Chaperone BiP', Nature, 353, 1991, pp. 726–730

[34] Corsi, A. K. and Schekman, R.: 'The Lumenal Domain of Sec63p Stimulates the ATPase Activity of BiP and Mediates BiP Recruitment to the Translocon in *Saccharomyces cerevisiae*', J. Cell Biol., 137, (7), 1997, pp. 1483–1493

[35] Liebermeister, W., Rapoport, T. A., and Heinrich, R.: 'Ratcheting in Posttranslational Protein Translocation: A Mathematical Model', J. Mol. Biol., 305, (3), 2001, pp. 643–656

[36] Elston, T.: 'The Brownian Ratchet and Power Stroke Models for Posttranslational Protein Translocation into the Endoplasmic Reticulum', Biophys. J., 82, (3), 2002, pp. 1239–1253

[37] Chauwin, J., Oster, G., and Glick, B.: 'Strong Precursor-Pore Interactions Constrain Models for Mitochondrial Protein Import', Biophys. J., 74, 1998, pp. 1732–1743

[38] Misselwitz, B., Staeck, O., and Rapaport, T. A.: 'J-Proteins Catalytically Activate Hsp70 Molecules to Trap a Wide Range of Peptide Sequences', Mol. Cell, 2, (5), 1998, pp. 593–603

[39] Misselwitz, B., Staeck, O., Matlack, K. E. S., and Rapaport, T. A.: 'Interaction of BiP with the J-Domain of the Sec63p Component of the Endoplasmic Reticulum Protein Translocation Complex', J. Biol.Chem., 274, (29), 1999, pp. 20110–20115

[40] Mayer, M., Reinstein, J., and Buchner, J.: 'Modulation of the ATPase Cycle of BiP by Peptides and Proteins', J. Mol. Biol., 330, 2003, pp. 137–144

[41] Kabani, M., Beckerich, J., and Gaillardin, C.: 'Sls1p Stimulates Sec63p-

Mediated Activated of Kar2p in a Conformation-Dependent Manner in the Yeast Endoplasmic Reticulum', Mol. Cell. Biol., 20, 2000, pp. 6923–6935

[42] de Keyzer, J., Steel, G., Hale, S., Humphries, D., and Stirling, C.: 'Nucleotide Binding by Lhs1p is Essential for Its Nucleotide Exchange Activity and for Function *In Vivo*', J. Biol. Chem., 284, 2009, pp. 31564–31571

[43] Levi, V. and Gratton, E.: 'Exploring Dynamics in Living Cells by Tracking Single Particles', Cell Biochem. Biophys., 48, 2007, pp. 1–15

[44] Liberek, K., Marszalek, J., Georgopoulos, C., and Zylicz, M.: ' *Escherichia coli* DnaJ and GrpE Heat Shock Proteins Jointly Stimulate ATPase Activity of DnaK', Proc. Natl. Acad. Sci., 88, 1991, pp. 2874–2878

[45] Blond-Elguindi, S., Dower, W., Lipshutz, R., Sprang, S., Sambrook, J., and Geiting, M.-J. H.: 'Affinity Panning of a Library of Peptides Displayed on Bacteriophages Reveals the Binding Specificity of BiP', Cell, 75, (4), 1993, pp. 717–728

[46] Rudiger, S., Buchberger, A., and Bukau, B.: 'Interaction of Hsp70 Chaperones with Substrates', Nat. Struct. Biol., 4, 1997, pp. 342–349

[47] Matlack, K., Misselwitz, B., Plath, K., and Rapoport, T.: 'BiP Acts as a Molecular Ratchet during Posttranslational Transport od Prepro-α Factor across the ER Membrane', Cell, 97, 1994, pp. 553–564

[48] Bernales, S., McDonald, K. L., and Walter, P.: 'Autophagy Counterbalances Endoplasmic Reticulum Expansion during the Unfolded Protein Response', PLoS Biol., 4, (12), 2006, pp. 2311–2324

[49] Craig, E. A., Huang, P., Aron, R., and Andrew, A.: 'The Diverse Roles of J-Proteins: The Obligate Hsp70 Co-chaperone', Rev. Physiol. Biochem. Pharmacol., 156, 2006, pp. 1–21

[50] Römisch, K.: 'Surfing the Sec61 Channel: Bidirectional Protein Translocation Across the ER Membrane', Journal of Cell Science, 112, 1999, pp. 4185–4191

[51] Rose, M. D., Misra, L. M., and Vogel, J. P.: 'Kar2, a Karyogamy Gene, is the Yeast Homologue of the Mammalian BiP/Grp78 Gene', Cell, 57, 1989, pp. 1211–1221

[52] Craven, R. A., Egerton, M., and Stirling, C. J.: 'A Novel Hsp70 of the Yeast ER Lumen is Required for the Efficient Translocation of a Number of Protein Precursors', EMBO J., pp. 2640–2650

[53] Feldheim, D., Rothblatt, J., and Schekman, R.: 'Topology and Functional Domains of Sec63p, an Endoplasmic Reticulum Membrane Protein Required for Secretory Protein Translocation', Mol. Cell Biol., 12, 1992, pp. 3288–3296

[54] Rothblatt, J. A., Deshaies, R. J., Sanders, S. L., Daum, G., and Schekman, R.: 'Multiple Genes are Required for Proper Insertion of Secretory Proteins into the Endoplasmic Reticulum of Yeast', J. Cell Biol., 109, 1989, pp. 2641–2652

[55] Brodsky, J. L., Goeckeler, J., and Schekman, R.: 'BiP and Sec63p are Required for Both Co- and Post-translational Protein Translocation into the Yeast Endoplasmic Reticulum', Proc. Natl. Acad. Sci., 92, 1995, pp. 9643–9646

[56] Brenan, K. E., Campbell, S. L., and Petzold, L. R.: 'The Numerical Solution of Initial Value Problems and Differential-Algebraic Equations',

[57] Fewell, S. W., Travers, K., Weissman, J. S., and Brodsky, J. L.: 'The Action of of Molecular Chaperones in the Early Secretory Pathway', Ann. Rev. Gene., 35, (1), 2001, pp. 149–191

[58] Awad, W., Estrada, I., Shen, Y., and Hendershot, L.: 'BiP Mutants that are Unable to Interact with Endoplasmic Reticulum DnaJ Proteins Provide Insights into Interdomain Interactions in BiP', Proc. Natl. Acad. Sci. USA, 105, 2008, pp. 1164–1169

[59] Schuck, S., Prinz, W. A., Thorn, K. S., Voss, C., and Walter, P.: 'Membrane Expansion Alleviates Endoplasmic Reticulum Stress Independently of the Unfolded Protein Response', J. Cell Biol., 187, (4), 2009, pp. 525–536

[60] Despa, F.: 'Dilation of the Endoplasmic Reticulum in Beta Cells Due to Molecular Crowding: Kinetic Simulations of Extension Limits and Consequences of Proinsulin Synthesis', Biophys. Chem., 140, (1-3), 2009, pp. 115–121

[61] Pierpaoli, E. V., Sandmeier, E., Schonfeld, H.-J., and Christen, P.: 'Control of the DnaK Chaperone Cycle by Substoichiometric Concentrations of the Co-chaperones DnaJ and GrpE', J. Biol. Chem., 273, (12), 1997, pp. 6643–6649

[62] Suh, W. C., Lu, C. Z., and Gross, C. A.: 'Structural Features Required for the Interaction of the Hsp70 Molecular Chaperone DnaK with the Co-chaperone DnaJ', J. Biol. Chem., 274, 1999, pp. 30534–30539

[63] Hindmarsh, A. C., Brown, P. N., Lee, S. L., Serban, R., and Woodward, C. S.: 'SUNDIALS: Suite of Nonlinear and Differential/Algebraic Solvers', ACM Trans. Math. Soft., 31, (3), 2005, pp. 363–396

[64] Stelling, J., Gilles, E. D., and III, F. J. D.: 'Robustness Properties of Circadian Clock Architectures', Proc. Natl. Acad. Sci. USA, 101, (36), 2004, pp. 13210–13215

[65] Johnson, A. and van Waes, M. A.: 'The Translocon: A Dynamic Gateway at the ER Membrane', Ann. Rev. Cell Biol., 15, 1999, pp. 799–842

[66] Beck, M., Förster, F., Ecke, M., Plitzko, J. M., Melchior, F., Gerisch, G., Baumeister, W., and Medalia, O.: 'Nuclear Pore Complex Structure and Dynamics Revealed by Cryoelectron Tomography', Science, 306, (5700), 2004, pp. 1387–1390

Tables

State Number	State Name
X_1	BiP-ATP
X_2	BiP-Sec63-ATP
X_3	BiP-Sec63-U-ATP
X_4	BiP-Sec63-U-ADP
X_5	BiP-U-NEF-ADP
X_6	BiP-U-ATP
X_7	BiP-U-ADP

Table 1: List of state numbers and names for the core ODE model

	Diffusing Species	BiP -ATP	BiP -Sec63-ATP	BiP -Sec63-U-ATP	BiP -Sec63-U-ADP	BiP -NEF-U-ADP	BiP -U-ATP	BiP -U-ADP
1	BiP U NEF	ML	M	M	M	ML	ML	ML
2	BiP Sec63 NEF, U	ML	ML	ML	ML	ML	ML	ML
3	BiP NEF, U Sec63=0	ML				ML	ML	ML

Table 2: Matrix describing which states and species diffuse in each scenario. States that remain in the membrane-associated zone (M) are shaded in gray while those states that can diffuse into the lumen as well (ML) are unshaded. Black represents states that are not present in the scenario.

Species	Initial Population Range	Initial Concentration Range (mM)
BiP	10,000-1,000,000	0.55-55
Sec63	10,000-25,000	0.55-1.37
NEF	10,000-1,000,000	0.55-55
U	10,000-150,000	0.55-8.25

Table 3: Range of initial populations (and concentrations) for protein species

Parameter	Max $dG/d\mathbf{p}$	Min $dG/d\mathbf{p}$	Mean $dG/d\mathbf{p}$
k_5	2.67×10^{-1}	6.85×10^{-4}	5.53×10^{-2}
k_6	6.94×10^{-2}	1.27×10^{-4}	1.07×10^{-2}
k_4	5.30×10^{-2}	3.89×10^{-5}	7.81×10^{-3}
k_9	4.01×10^{-2}	8.44×10^{-9}	5.40×10^{-3}
k_7	1.35×10^{-2}	3.18×10^{-5}	2.26×10^{-3}
k_8	1.07×10^{-2}	4.67×10^{-6}	1.37×10^{-3}
k_3	6.21×10^{-3}	3.27×10^{-8}	9.59×10^{-4}
k_{-2}	5.54×10^{-3}	3.28×10^{-6}	6.27×10^{-4}
k_{-7}	2.93×10^{-3}	2.53×10^{-7}	5.70×10^{-5}
k_1	8.32×10^{-4}	1.67×10^{-7}	1.93×10^{-5}
k_{-3}	4.09×10^{-4}	1.61×10^{-8}	3.43×10^{-6}
k_2	4.85×10^{-5}	6.85×10^{-8}	2.68×10^{-6}
k_{-1}	6.74×10^{-7}	7.09×10^{-9}	1.54×10^{-8}

Table 4: Scaled sensitivities of the BiP ratio ranked by maximum value for 13 sets of BiP initial conditions in the range of 0.55 to 55 mM.

Figure Captions

Figure 1. Molecular chaperone BiP/Kar2 is required for efficient protein translocation into the ER lumen, protein folding and maturation, and ER-associated degradation (ERAD). Interactions with selective co-chaperones include membrane protein Sec63 and freely diffusing Scj1 and Jem1. Intrinsic rates of peptide release are low; thus following ATP hydrolysis, nucleotide exchange is facilitated by Sil1 or Lhs1. In this illustration, Sec61 is a member of the ER membrane pore complex responsible for translocation and possibly the transport of aberrant proteins by ERAD.

Figure 2. Schematic of our ODE model consisting of 7 states that represent the interactions of BiP with co-chaperone Sec63, nascent and unfolded proteins (U), nucleotide exchange factors (NEF) Sil1 and Lhs1, and required energy components ATP and ADP.

Figure 3. The PDE model consists of a membrane-associated zone and lumen represented by reaction-diffusion equations. The length of the membrane-associated zone, L_z, was taken to be 35 nm, while the annular radius of the lumen, L_l, is 110 nm ([65, 66]; Supplementary Material).

Figure 4. Log-log plots for Scenario 1 (Sec63 is tethered to the membrane) detailing the BiP ratio (total BiP concentration on the membrane divided by the total BiP concentration in the lumen) for total BiP varying from 0.55 to 55 mM (10^4 to 10^6 molecules) for the modified ODE (left) and PDE (right) models. The graphs show three sets of different total Sec63 concentrations (corresponding to 10,000, 17,700, and 25,000 molecules). When Sec63 is allowed to diffuse (Scenario 2) or is removed from the system (Scenario 3), the BiP ratio is uniformly one.

Figure 5. Log-log plot of the BiP ratio in the wild-type scenario for a variation in total BiP and U, while fixing Sec63 = 0.97 mM. The graph shows six sets of different total U population (from 0.55 to 8.25 mM).

Figure 6. Log-log plot of the BiP ratio for variation in the Sec63-dependent (k_2) and Sec63-independent BiP-U association rate (k_7) from 3.5×10^4 to $3.5 \times 10^8 M^{-1}s^{-1}$ and 8.3×10^1 to $8.3 \times 10^5 M^{-1}s^{-1}$, respectively.

Figure 7. Log-log plot of the BiP ratio for variation in Sec63 dissociation rate (k_5,k_{-3}) from 0.0086 to 8.6 s^{-1} and 0.038 to 38 s^{-1}, respectively.

Figure 8. Histograms of the BiP ratio for 10^4, 10^5,and 10^6 BiP molecules (0.55, 5.5, and 55 mM, respectively) while varying all kinetic parameters simultaneously.

Figures

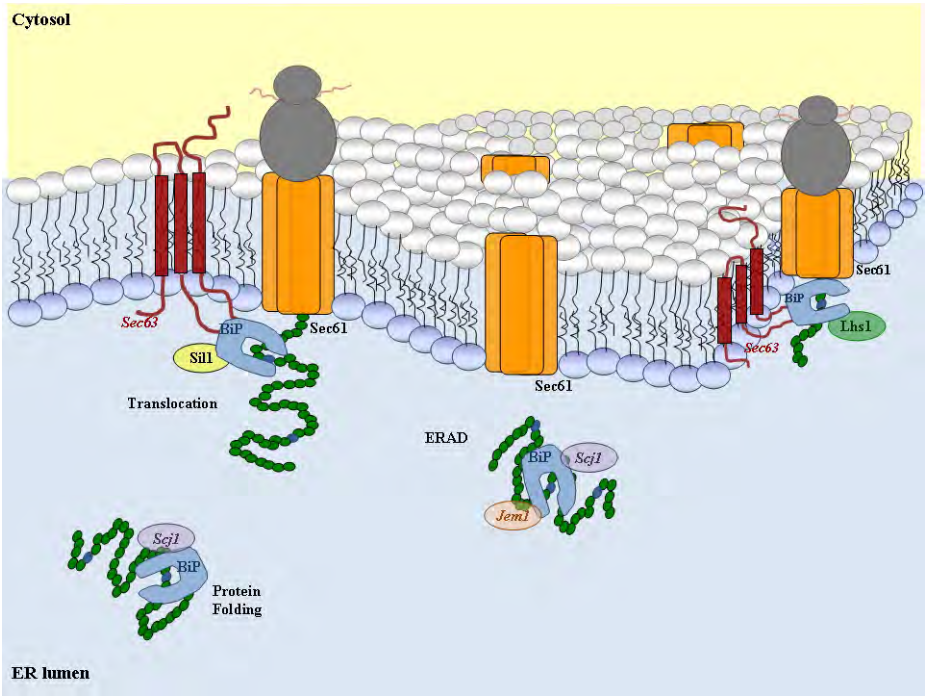

Figure 1: Molecular chaperone BiP/Kar2 is required for efficient protein translocation into the ER lumen, protein folding and maturation, and ER-associated degradation (ERAD). Interactions with selective co-chaperones include membrane protein Sec63 and freely diffusing Scj1 and Jem1. Intrinsic rates of peptide release are low; thus following ATP hydrolysis, nucleotide exchange is facilitated by Sil1 or Lhs1. In this illustration, Sec61 is a member of the ER membrane pore complex responsible for translocation and possibly the transport of aberrant proteins by ERAD.

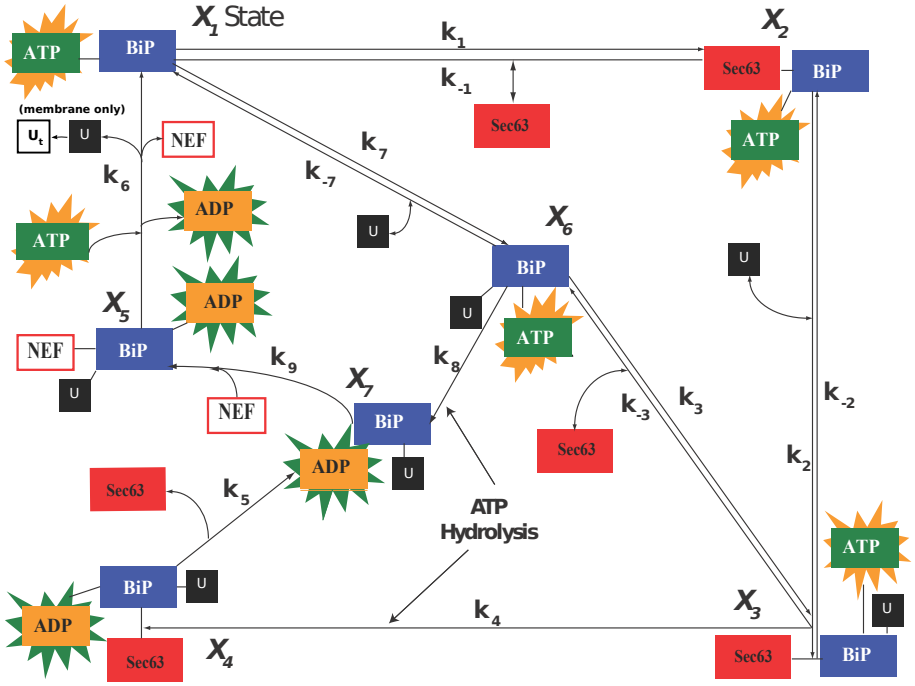

Figure 2: Schematic of our ODE model consisting of 7 states that represent the interactions of BiP with co-chaperone Sec63, nascent and unfolded proteins (U), nucleotide exchange factors (NEF) Sil1 and Lhs1, and required energy components ATP and ADP.

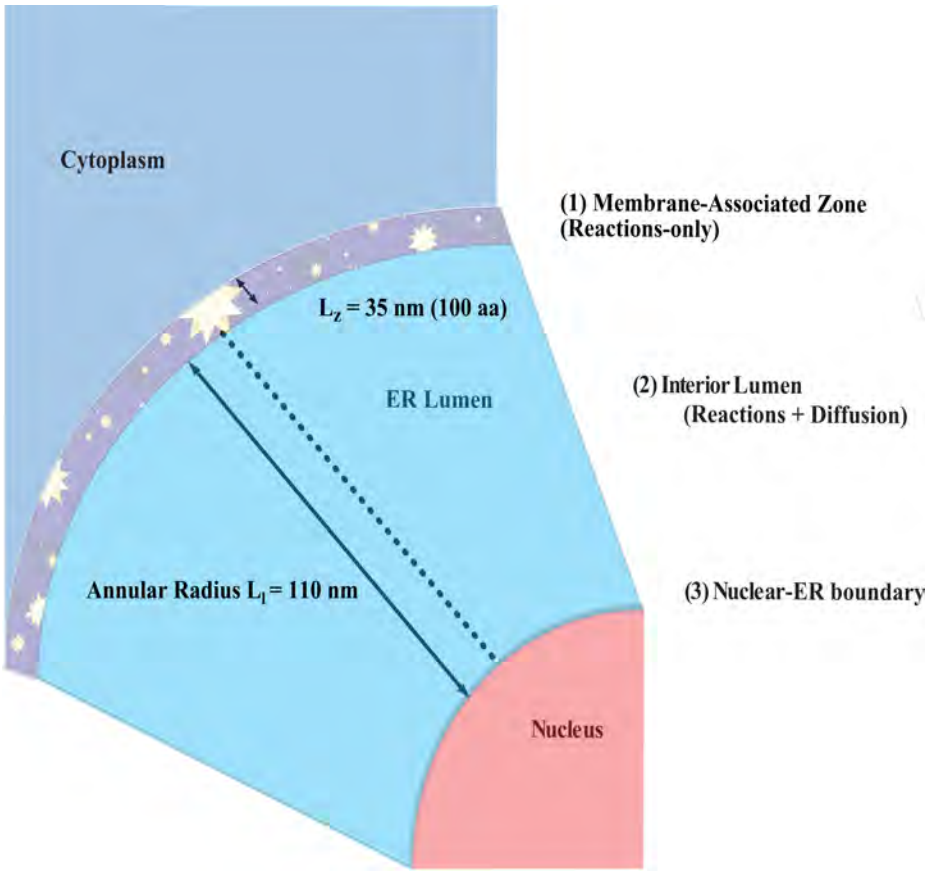

Figure 3: The PDE model consists of a membrane-associated zone and lumen represented by reaction-diffusion equations. The length of the membrane-associated zone, L_z, was taken to be 35 nm, while the annular radius of the lumen, L_l, is 110 nm ([65, 66]; Supplementary Material).

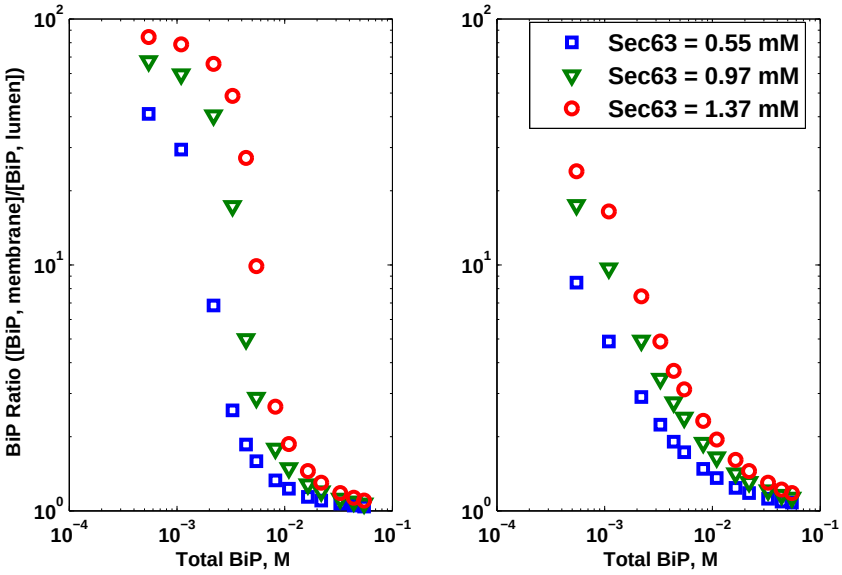

Figure 4: Log-log plots for Scenario 1 (Sec63 is tethered to the membrane) detailing the BiP ratio (total BiP concentration on the membrane divided by the total BiP concentration in the lumen) for total BiP varying from 0.55 to 55 mM (10^4 to 10^6 molecules) for the modified ODE (left) and PDE (right) models. The graphs show three sets of different total Sec63 concentrations (corresponding to 10,000, 17,700, and 25,000 molecules). When Sec63 is allowed to diffuse (Scenario 2) or is removed from the system (Scenario 3), the BiP ratio is uniformly one.

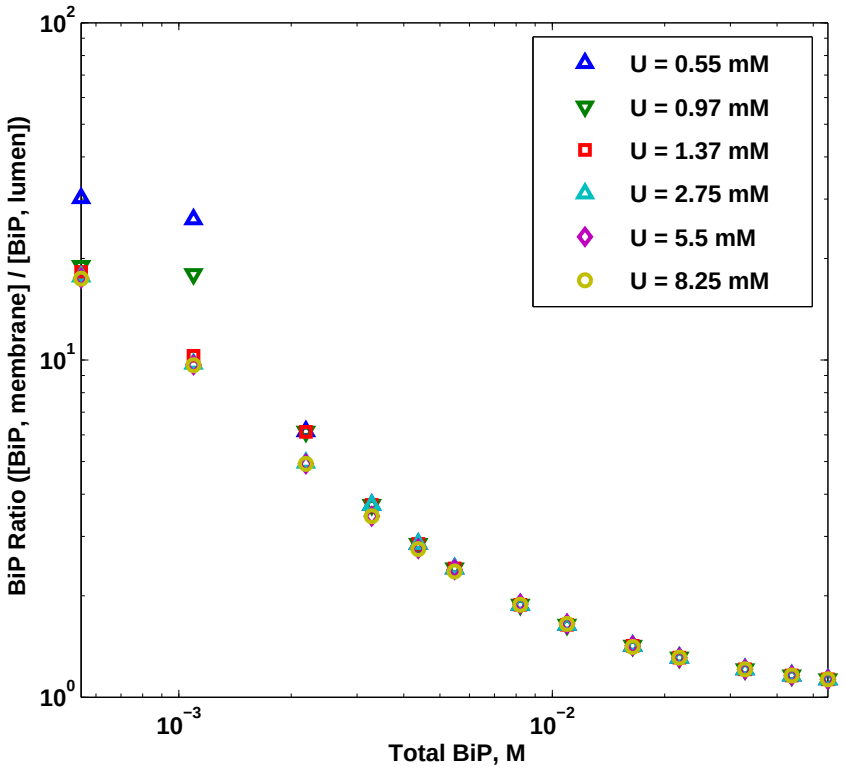

Figure 5: Log-log plot of the BiP ratio in the wild-type scenario for a variation in total BiP and U, while fixing Sec63 = 0.97 mM. The graph shows six sets of different total U population (from 0.55 to 8.25 mM).

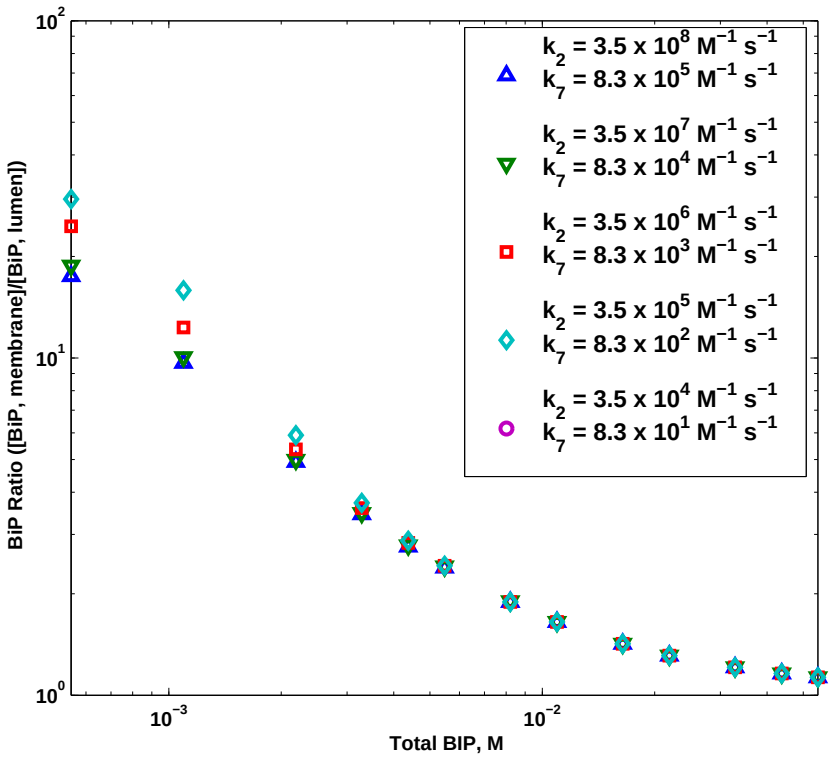

Figure 6: Log-log plot of the BiP ratio for variation in the Sec63-dependent (k_2) and Sec63-independent BiP-U association rate (k_7) from 3.5×10^4 to $3.5 \times 10^8 M^{-1}s^{-1}$ and 8.3×10^1 to $8.3 \times 10^5 M^{-1}s^{-1}$, respectively.

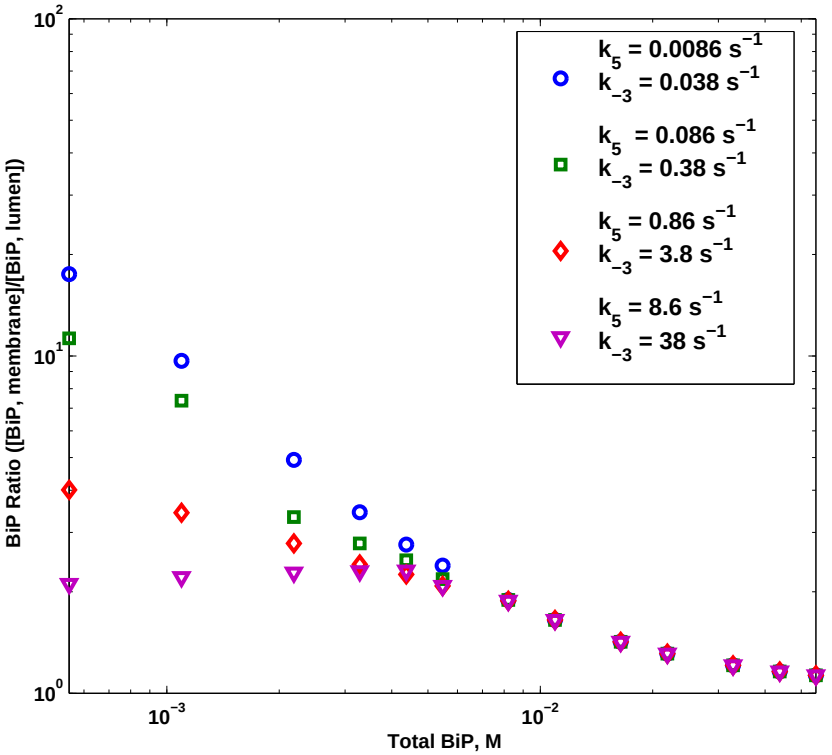

Figure 7: Log-log plot of the BiP ratio for variation in Sec63 dissociation rate (k_5,k_{-3}) from 0.0086 to 8.6 s^{-1} and 0.038 to 38 s^{-1}, respectively.

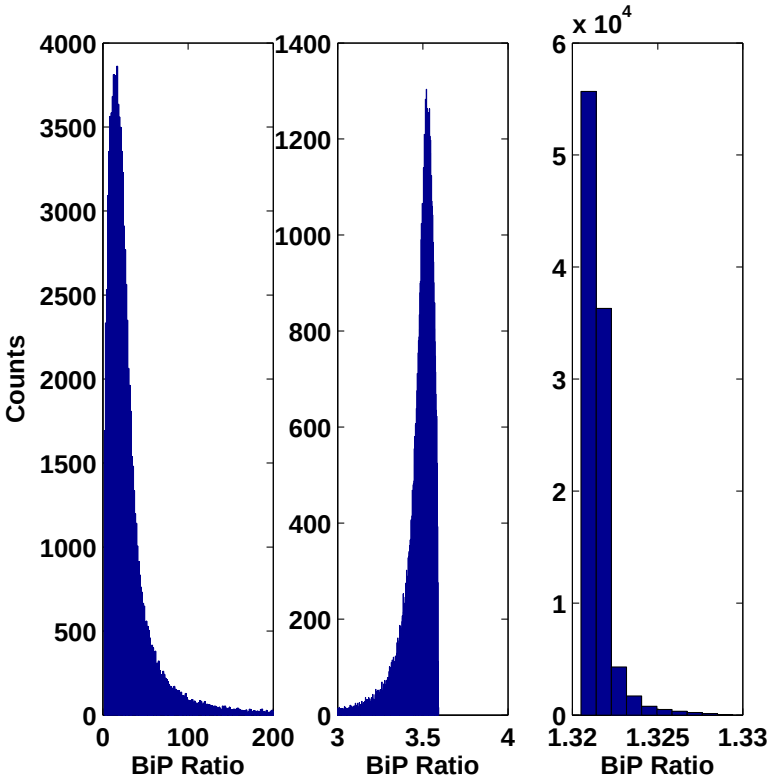

Figure 8: Histograms of the BiP ratio for 10^4, 10^5,and 10^6 BiP molecules (0.55, 5.5, and 55 mM, respectively) while varying all kinetic parameters simultaneously.

Supplementary Material

S1 Estimations

S1.1 Spatial Parameters

Johnson and colleagues have demonstrated that BiP seals the translocation pore until the translocating peptide extends 50 amino acids into the ER lumen. This observation corresponds to a peptide that extends 17.5 nm (0.35 nm per residue) from the translocation pore into the ER lumen. We have approximated a two-fold increase in the depth of the membrane-associated reaction zone, defined as the regime where BiP, U, and Sec63 are interactive, resulting in a length L_z of 35 nm.

We could not find a referenced value for the annular radius of the ER lumen. However, we believe it is justified to use the dimensions of the nuclear pore complex (NPC). The NPC functions as a conduit for molecular transport from the cytosol to the nucleus, and thus spans the depth of the ER. Based on studies of NPC structure , a value of 110 nm served as an estimate for the length L_l of the ER lumen.

The diffusion rate D for all species was set to the measured value of 0.45 $\mu m^2/s$ from fluorescence photobleaching (FRAP) measurements of GFP-tagged VSVG protein .

S1.2 Kinetic Rate Constants

- k_1 for the binding of BiP to Sec63 was set to $2.44 \times 10^4\ M^{-1}s^{-1}$, based on the interaction between heat shock proteins DnaK and DnaJ in *E. coli* .
- k_{-1} for the dissociation of BiP from Sec63 was set to 0.0012 s^{-1}, based on the same experiments for determining k_1 .
- k_2 for the Sec63-activated BiP binding with the unfolded protein was estimated to be $3.51 \times 10^8\ M^{-1}s^{-1}$, based on fitting of data to the Brownian ratchet model with the protein ppαF interacting with BiP .
- k_{-2} is the corresponding dissociation rate to k_2 using the same method, and was estimated to be 0.0277 s^{-1} .
- k_3, describing Sec63's association with the BiP-U-ATP complex, was calculated to be $1.9 \times 10^2\ M^{-1}s^{-1}$, based on the literature value for k_{-3} and the equilibrium constant of 200 μM. This was based on BiP binding with a synthetic hydrophobic peptide p15 in the presence of ATP .
- k_{-3}, describing the dissociation of Sec63 from BiP bound to unfolded protein in the presence of ATP, was taken to be 0.038 s^{-1}. This was based on BiP binding synthetic hydrophobic peptide p15 .
- k_4, representing the hydrolysis of the trimeric complex BiP-U-Sec63, was estimated to be 0.016 s^{-1}, based on the measured rate between murine BiP and the heptapeptide HD14 without the co-chaperone .
- k_5 was estimated to be 0.0086 s^{-1} for the dissociation of Sec63 from BiP and U in the presence of ADP .

- k_6 was estimated to be $5.3 \times 10^5\ M^{-1}s^{-1}$ from the association of human Hsp70 and murine nucleotide exchange factor BAG-1 in the absence of peptide .
- k_7 representing the association of BiP and substrate in the presence of ATP was estimated to be $8.3 \times 10^5\ M^{-1}s^{-1}$ as calculated from fitting translocation time-course data to a Brownian ratchet model at a BiP concentration of $1\mu M$.
- k_{-7} for the dissociation of BiP and substrate (in the presence of ATP) was estimated to be 0.0277 s^{-1}, identical to k_{-2} .
- k_8 for the hydrolysis of the BiP-U complex was taken to be 0.016 s^{-1}, the same as rate k_4 .
- k_9 for the dissociation of BiP from NEF and U was estimated to be 0.267 s^{-1} from a similar interaction with human Hsp70 and murine nucleotide exchange factor BAG-1 in the absence of peptide .

S2 Notes

Unfolded proteins are defined as one species in the model; however, slightly different reactions involving them occur in the membrane-associated zone (M) and the lumen (L). In the former location, the loss of proteins at the translocon due to completed translocation (reaction 6 in Table S1, $U \rightarrow U_t$) is offset by a creation reaction ($\emptyset \rightarrow U$) to ensure a continual flux of proteins. The differential equation for free U therefore has two terms that cancel (Table S2). In the lumen, the outcome of reaction 6 is to return bound unfolded protein to the free pool; there is no offsetting production reaction.

.

References

Johnson, A. and van Waes, M. A.: 'The Translocon: A Dynamic Gateway at the ER Membrane', Ann. Rev. Cell Biol., 15, 1999, pp. 799–842

Beck, M., Förster, F., Ecke, M., Plitzko, J. M., Melchior, F., Gerisch, G., Baumeister, W., and Medalia, O.: 'Nuclear Pore Complex Structure and Dynamics Revealed by Cryoelectron Tomography', Science, 306, (5700), 2004, pp. 1387–1390

Nehls, S., Snapp, E. L., Cole, N. B., Zaal, K. J. M., Kenworthy, A. K., Roberts, T. H., Ellenberg, J., Presley, J. F., Siggia, E., and Schwartz, J. L.: 'Dynamics and Retention of Misfolded Proteins in Native ER Membranes', Nature Cell Biol., 2, 2000, pp. 288–295

Mayer, M. P., Schröder, H., Rüdiger, S., Paal, K., and Bukau, B.: 'Investigation of the Interaction between DnaK and DnaJ by Surface Plasmon Resonance Spectroscopy', J. Mol. Biol., 289, 1999, pp. 1131–1134

Elston, T.: 'The Brownian Ratchet and Power Stroke Models for Posttranslational Protein Translocation into the Endoplasmic Reticulum', Biophys. J., 82, (3), 2002, pp. 1239–1253

Misselwitz, B., Staeck, O., and Rapaport, T. A.: 'J-Proteins Catalytically Activate Hsp70 Molecules to Trap a Wide Range of Peptide Sequences', Mol. Cell, 2, (5), 1998, pp. 593–603

Mayer, M., Reinstein, J., and Buchner, J.: 'Modulation of the ATPase Cycle of BiP by Peptides and Proteins', J. Mol. Biol., 330, 2003, pp. 137–144

Stuart, J., Myszeka, D., Joss, L., Mitchell, R., McDonald, S., Xie, Z., Takayama, S., Reed, S., and Ely, K.: 'Characterization of Interactions Between the Anti-Apopotic Protein BAG-1 and Hsc70 Molecular Chaperones', J. Biol. Chem., 273, 1998, pp. 22506–22514

Liebermeister, W., Rapoport, T. A., and Heinrich, R.: 'Ratcheting in Post-translational Protein Translocation: A Mathematical Model', J. Mol. Biol., 305, (3), 2001, pp. 643–656

Tables

	Reaction (Species)	Reaction (States)	Kinetic Rate	Ref.
1	BiP-ATP + Sec63 ↔ BiP-Sec63-ATP	X1 + Sec63 ↔ X2	$k_1 = 2.44 \times 10^4\ M^{-1}\ s^{-1}$ $k_{-1} = 0.0012\ s^{-1}$	
2	BiP-Sec63-ATP + U ↔ BiP-Sec63-U-ATP	X2 + U ↔ X3	$k_2 = 3.51 \times 10^8\ M^{-1}\ s^{-1}$ $k_{-2} = 0.0277\ s^{-1}$	[]
3	BiP-U-ATP + Sec63 ↔ BiP-Sec63-U-ATP	X6 + Sec63 ↔ X3	$k_3 = 1.9 \times 10^2\ M^{-1}\ s^{-1}$ $k_{-3} = 0.038\ s^{-1}$	
4	BiP-Sec63-U-ATP → BiP-Sec63-U-ADP + Pi	X3 → X4 + Pi	$k_4 = 0.016\ s^{-1}$	
5	BiP-Sec63-U-ADP → BiP-U-ADP + Sec63	X4 → X7 + Sec63	$k_5 = 0.0086\ s^{-1}$	
6	BiP-U-NEF-ADP → BiP-ATP + U_t + NEF	X5 → X1 + NEF + U_t	$k_6 = 0.267\ s^{-1}$	[]
7	BiP-ATP + U ↔ BiP-U-ATP	X1 + U ↔ X6	$k_7 = 8.3 \times 10^5\ M^{-1}\ s^{-1}$ $k_{-7} = 0.0277\ s^{-1}$	[,]
8	BiP-U-ATP → BiP-U-ADP + Pi	X6 → X7 + Pi	$k_8 = 0.016\ s^{-1}$	[]
9	BiP-U-ADP + NEF → BiP-U-NEF-ADP	X7 + NEF → X5	$k_9 = 5.3 \times 10^5\ M^{-1}\ s^{-1}$	
10	$\emptyset \rightarrow$ U	$\emptyset \rightarrow$ U	$k_6[X5]$	[]

Table S1: Reaction list for the core ODE model

$$
\begin{aligned}
\frac{d[X_1]}{dt} &= -k_1[X_1][Sec63] + k_{-1}[X_2] - k_7[X_1][U] + k_{-7}[X_6] + k_6[X_5] \\
\frac{d[X_2]}{dt} &= k_1[X_1][Sec63] - k_{-1}[X_2] - k_2[X_2][U] + k_{-2}[X_3] \\
\frac{d[X_3]}{dt} &= k_2[X_2][U] - k_{-2}[X_3] + k_3[X_6][Sec63] - k_{-3}[X_3] - k_4[X_3] \\
\frac{d[X_4]}{dt} &= k_4[X_3] - k_5[X_4] \\
\frac{d[X_5]}{dt} &= k_9[X_7][NEF] - k_6[X_5] \\
\frac{d[X_6]}{dt} &= k_7[X_1][U] - k_{-7}[X_6] - k_3[X_6][Sec63] + k_{-3}[X_3] - k_8[X_6] \\
\frac{d[X_7]}{dt} &= k_8[X_6] + k_5[X_4] - k_9[X_7][NEF] \\
\frac{d[NEF]}{dt} &= k_6[X_5] - k_9[X_7][NEF] \\
\frac{d[Sec63]}{dt} &= -k_1[X_1][Sec63] - k_3[X_6][Sec63] + k_{-1}[X_2] + k_{-3}[X_3] + k_5[X_4] \\
\frac{d[U]}{dt} &= -k_7[X_1][U] + k_{-7}[X_6] - k_2[X_2][U] + k_{-2}[X_3] + \begin{cases} 0 & \text{M} \\ k_6[X_5] & \text{L} \end{cases}
\end{aligned}
$$

Table S2: Equations for the core ODE model. In the equation for free unfolded proteins (U), there are different terms for the membrane-associated (M) and lumenal (L) versions.